FERMILAB-PUB–98/146-T
IFT–98/23
CERN-TH/98-148

The Higgs Boson Mass as a Probe of the Minimal Supersymmetric Standard Model

M. Carena[1], P.H. Chankowski[2],
S. Pokorski[2,3], C.E.M. Wagner[3]

[1] Fermi National Accelerator Laboratory,
P.O. Box 500, Batavia, IL 60510, USA
[2] Institute of Theoretical Physics, Warsaw University
ul. Hoża 69, 00–681 Warsaw, Poland
[3] CERN, TH Division, CH-1211 Geneva 23, Switzerland.

June 15, 1998

Abstract

Recently, the LEP collaborations have reported a lower bound on a Standard Model-like Higgs boson of order 89 GeV. We discuss the implications of this bound for the minimal supersymmetric extension of the Standard Model (MSSM). In particular, we show that the lower bound on $\tan\beta$, which can be obtained from the presently allowed Higgs boson mass value, becomes stronger than the one set by the requirement of perturbative consistency of the theory up to scales of order M_{GUT} (associated with the infrared fixed-point solution of the top quark Yukawa coupling) in a large fraction of the allowed parameter space. The potentiality of future LEP2 searches to further probe the MSSM parameter space is also discussed.

One of the most striking predictions of the minimal supersymmetric extension of the Standard Model (the MSSM) is the existence of a light, $\mathcal{O}(100$ GeV), Higgs particle. The supersymmetric prediction for the range of the lighter CP-even Higgs boson mass is nicely consistent with the fits to the electroweak precision data (for recent fits see [1, 2]). However, the existence of the Higgs boson has not yet been directly established experimentally and the search for it continues to be the main goal of LEP2. The absence of such a light Higgs particle would eventually rule out low energy supersymmetry in its minimal version. The present experimental lower bound for its mass enters into the region most relevant for the MSSM. It is, therefore, quite timely to discuss the constraints on the MSSM derived from the present and near-future expected lower bounds on the Higgs boson mass M_h or by the potential discovery of a light Higgs boson with a mass M_h. One of the most interesting aspects of this question is the lower bound on the parameter $\tan\beta$ ($\tan\beta = v_2/v_1$, where v_1 and v_2 are the two Higgs boson doublet vacuum expectation values), which can be derived within this context. Considering the MSSM as a low-energy effective theory, the bounds on $\tan\beta$ depend on the physical stop masses (and their mixing angle) but do not depend on any theoretical assumption, e.g. on the pattern of soft terms at the GUT scale, or, more generally, on the actual mechanism that communicates supersymmetry breaking to the observable sector.

Supersymmetric extensions of the Standard Model provide a framework for a consistent link between low-energy physics and physics at the GUT scale. Since the top Yukawa coupling is not asymptotically free, the requirement of perturbative consistency of the theory up to the scale M_{GUT} puts a strong and very interesting bound on the top-quark Yukawa coupling at the scale of the top-quark mass, $h_t(m_t)$ [3]. The bound depends slightly on the mass spectrum of the MSSM and can be somewhat altered by the presence of extra matter, e.g. $\mathbf{5} + \bar{\mathbf{5}}$ vector-like multiplets at some intermediate scale M_I. With the measured value $m_t^{pole} = 173.9 \pm 5.2$ GeV [4], and by using the relation

$$m_t^{pole} = \frac{1}{\sqrt{2}} h_t(m_t) v \sin\beta + ... \tag{1}$$

(where $v^2 \equiv v_1^2 + v_2^2 = 4M_W^2/(g'^2 + g^2) + ...$, and the ellipses stand for perturbative corrections), the upper bound on $h_t(m_t)$ can also be translated into a lower bound on $\tan\beta$.

In this letter we compare the bounds on $\tan\beta$ obtained for a given value of M_h within the low-energy MSSM with the bound on $\tan\beta$ derived from the requirement of perturbative consistency of the theory up to the scale M_{GUT}. We shall show that even the present experimental limit on M_h implies a bound on $\tan\beta$, which is well above the perturbativity bound for a large range of stop masses (and mixings). The infrared fixed-point scenario, associated

with the values of the top-quark Yukawa coupling close to the perturbative upper bound remains consistent with the present limit on M_h only for large values of the heavier stop mass, large stop mass splitting and large mixing angle.

Stronger lower bounds on M_h imply more stringent lower bounds on $\tan\beta$, which are consistent with the infrared fixed-point scenario only for heavier and heavier stops; eventually the two bounds no longer intersect each other. This is consistent with the well-known upper bound on M_h obtained in the infrared fixed-point scenario in the minimal supergravity model, with universal soft SUSY-breaking terms at the GUT scale. As shown in ref. [5] (and recently confirmed in a further study [6]), in this case $M_h \lesssim 98$ GeV for $M_{\tilde{t}_i} \lesssim 1$ TeV, where $M_{\tilde{t}_i}$ are the physical stop masses. Our general analysis shows that in the unconstrained low-energy MSSM the above limit can only be slightly relaxed, by at most a few GeV. For instance, $M_h \simeq 103$ GeV is consistent with the infrared fixed point of h_t for stop masses of the order of 1 TeV, but only for very large and positive values of the stop mixing angle and/or a top mass close to its upper 1σ range.

In general, taking into account the full structure of the stop mass matrix, the lighter CP-even Higgs boson mass in the MSSM is parametrized by

$$M_h = M_h\left(M_A, \tan\beta, m_t, M_{\tilde{t}_1}, M_{\tilde{t}_2}, A_t, \mu, ...\right) \tag{2}$$

where A_t and μ determine the mixing angle of the stops (as well as some of their trilinear couplings to the Higgs bosons) and the ellipses stand for other parameters whose effects are not dominant (e.g. the gaugino mass parameters, or the sbottom sector parameters, which become relevant only for large values of $\tan\beta > 10$).

The maximal M_h is always obtained for $M_A \gg M_Z$ (in practice, the bound is saturated for $M_A \gtrsim 250$ GeV). In this limit one gets from the effective potential approach (see ref. [7] for details) a particularly simple result for the one-loop corrected M_h [8]:

$$M_h^2 = M_Z^2 \cos^2 2\beta + \frac{3\alpha}{4\pi s_W^2}\frac{m_t^4}{M_W^2}\left[\log\left(\frac{M_{\tilde{t}_2}^2 M_{\tilde{t}_1}^2}{m_t^4}\right) + \left(\frac{M_{\tilde{t}_2}^2 - M_{\tilde{t}_1}^2}{4m_t^2}\sin^2 2\theta_{\tilde{t}}\right)^2\right.$$

$$\left. \times\, f(M_{\tilde{t}_2}^2, M_{\tilde{t}_1}^2) + \frac{M_{\tilde{t}_2}^2 - M_{\tilde{t}_1}^2}{2m_t^2}\sin^2 2\theta_{\tilde{t}} \log\left(\frac{M_{\tilde{t}_2}^2}{M_{\tilde{t}_1}^2}\right)\right] \tag{3}$$

where $f(x,y) = 2 - (x+y)/(x-y)\log(x/y)$. For large M_A, the dependence on the parameters A_t and μ always appears in the combination $\tilde{A}_t = A_t -$

$\mu/\tan\beta$, [1] through the dependence on the left–right stop mixing angle $\theta_{\tilde{t}}$,

$$\sin 2\theta_{\tilde{t}} = \frac{2m_t \tilde{A}_t}{M^2_{\tilde{t}_2} - M^2_{\tilde{t}_1}}. \tag{4}$$

The two-loop corrections to M_h are typically $\mathcal{O}(20\%)$ of the one-loop corrections and are negative [9]–[12]. They are taken into account in our numerical results (we use the method proposed in [11]). Eq. (3) is, however, very useful for the qualitative understanding of the final results. As can be seen from Eq. (3), for a given lower limit on M_h, larger values of the radiative corrections to M_h are required for lower values of $\tan\beta$ (i.e. for smaller values of the tree level part of M_h^2). Thus, maximizing the radiative corrections to M_h sets a lower bound on $\tan\beta$ as a function of $M_{\tilde{t}_1}$, $M_{\tilde{t}_2}$ and $\sin 2\theta_{\tilde{t}}$. It is hence interesting to analyse the dependence of Eq. (3) on $\sin 2\theta_{\tilde{t}}$.

For fixed $M_{\tilde{t}_1}$, $M_{\tilde{t}_2}$, the mass of the lighter CP-even Higgs boson is a quadratic function of $\sin^2 2\theta_{\tilde{t}}$,

$$M_h^2 = F(M_{\tilde{t}_i}) + G(M_{\tilde{t}_i}) \sin^2 2\theta_{\tilde{t}} + H(M_{\tilde{t}_i}) \sin^4 2\theta_{\tilde{t}}, \tag{5}$$

with $G(M_{\tilde{t}_i}) > 0$ and $H(M_{\tilde{t}_i}) < 0$. Hence, there is a maximum value of M_h^2, which is obtained for

$$\left(\sin^2 2\theta_{\tilde{t}}\right)^{\max} = \frac{-4\, m_t^2 \log\left(M^2_{\tilde{t}_2}/M^2_{\tilde{t}_1}\right)}{2\left(M^2_{\tilde{t}_2} - M^2_{\tilde{t}_1}\right) - \left(M^2_{\tilde{t}_2} + M^2_{\tilde{t}_1}\right)\log\left(M^2_{\tilde{t}_2}/M^2_{\tilde{t}_1}\right)}. \tag{6}$$

For small values of the stop mass splitting, the value of $\sin^2 2\theta_{\tilde{t}}$ that is obtained from the above expression is larger than 1. Indeed, when the difference between the stop masses is much smaller than their sum,

$$\left(\sin^2 2\theta_{\tilde{t}}\right)^{max} \simeq \frac{12 m_t^2 \left(M^2_{\tilde{t}_2} + M^2_{\tilde{t}_1}\right)}{\left(M^2_{\tilde{t}_2} - M^2_{\tilde{t}_1}\right)^2}. \tag{7}$$

In these cases the physical value of the Higgs boson mass takes its maximal value for $\sin^2 2\theta_{\tilde{t}} = 1$, that is for equal values of the diagonal entries $M^2_{\tilde{t}_R}$, $M^2_{\tilde{t}_L}$, of the stop square mass matrix. Moreover, in such cases, zero mixing angle represents a minimum of the Higgs boson mass value.

For $\sin^2 2\theta_{\tilde{t}} = 1$ the stop masses are given by $M^2_{\tilde{t}_{1,2}} = M^2_{\rm SUSY} \mp m_t \tilde{A}_t$, where $M^2_{SUSY} = M^2_{\tilde{t}_L} = M^2_{\tilde{t}_R}$. In this case, it is possible to get a simple expression for M_h^2 including the dominant two-loop leading-logarithmic corrections, written

[1] The quoted formula stays valid even in the case that A_t and/or μ develop complex phases, provided $\tilde{A}_t$ is replaced everywhere by $|\tilde{A}_t| \equiv |A_t - \mu^*/\tan\beta|$.

in terms of $\tilde{A}_t$ and M_{SUSY}. In the limit $(m_t \tilde{A}_t)/M^2_{\rm SUSY} \ll 1$, it is given by [11]

$$\begin{aligned} M_h^2 &\simeq M_Z^2 \cos^2 2\beta \left(1 - \frac{3}{8\pi^2}\frac{m_t^2}{v^2} L_t\right) \\ &+ \frac{3}{4\pi^2}\frac{m_t^4}{v^2}\left[\frac{1}{2}\tilde{X}_t + L_t + \frac{1}{16\pi^2}\left(\frac{3}{2}\frac{m_t^2}{v^2} - 8g_3^2\right)\left(\tilde{X}_t L_t + L_t^2\right)\right], \end{aligned} \quad (8)$$

where $L_t \equiv \log\left(M^2_{\rm SUSY}/m_t^2\right)$,

$$\tilde{X}_t = \frac{2\tilde{A}_t^2}{M^2_{\rm SUSY}}\left(1 - \frac{\tilde{A}_t^2}{12 M^2_{\rm SUSY}}\right) \quad (9)$$

and m_t and $g_3^2 \equiv 4\pi\alpha_3$ are the running top mass and the strong gauge coupling evaluated at the scale m_t, respectively. The expression (8) for M_h^2 has a maximum at $\tilde{A}_t = \sqrt{6} M_{\rm SUSY}$. Thus, for moderate values of the stop mass splitting, the Higgs boson mass is maximized by keeping equal values of the diagonal entries in the stop mass matrix ($M^2_{\tilde{t}_R} \approx M^2_{\tilde{t}_L}$) and is approximately given by Eq. (8).

For sufficiently large values of the stop mass splitting, the value of $(\sin 2\theta_{\tilde{t}})^{max}$ given by Eq. (6) becomes lower than 1. Even in these cases, the maximal Higgs boson mass is obtained for rather large values of $\tilde{A}_t$. To see this we can take, for example, the case in which the heavier stop mass is of order 1 TeV and the lighter stop mass is of the order of the top quark mass. From Eq. (6) we get

$$\left(\sin^2 2\theta_{\tilde{t}}\right)^{max} \simeq 10 \frac{m_t^2}{M^2_{\tilde{t}_2}}, \quad (10)$$

corresponding to a value of $|\sin 2\theta_{\tilde{t}}| \simeq 0.6$. Comparing the above expression with Eq. (4), we get

$$|\tilde{A}_t| \simeq 1.5 M_{\tilde{t}_2}. \quad (11)$$

Hence, as stated above, large values of $\tilde{A}_t$ are necessary to maximize M_h^2, even in the case of very large splitting of the stop masses. From the value of $\sin 2\theta_{\tilde{t}}$ it is also clear that in this case the splitting in the left- and right-handed stop masses is crucial for generating the difference in physical masses of the heavier and lighter stops.

The computation of the Higgs boson mass is still affected by theoretical uncertainties, most notably, those associated with the two-loop finite threshold corrections to the effective quartic couplings of the Higgs potential. Recently, partial diagrammatic two-loop computation of the Higgs mass has been performed [13]. Taking the appropriate limit, the values obtained by this method are in agreement with our results within a range of 2-3 GeV. We take these differences as the estimates of the uncertainty of the computed

M_h. In order to take this uncertainty into account and to remain on the conservative side, in all cases discussed below we have lowered the bound by 2 GeV with respect to the actually considered Higgs boson mass limit. We have also considered low values of the chargino and neutralino masses (of the order of 200 GeV) to minimize their negative effects on the Higgs masses.

Our numerical results are shown in Figs. 1–3. In Fig. 1, we plot the lower bounds on $\tan\beta$, following from the present experimental limit of 89.5 GeV [14] on a Standard Model (SM)-like Higgs boson mass ($M_A \gtrsim 250$ GeV) [2], as a function of $M_{\tilde{t}_2}$ (the heavier stop mass) for several values of the stop mass splitting $\Delta M_{\tilde{t}} \equiv M_{\tilde{t}_2} - M_{\tilde{t}_1}$. For a given $M_{\tilde{t}_2}$ and $\Delta M_{\tilde{t}}$, a scan over $\sin\theta_{\tilde{t}}$ is performed in order to find the lowest value of $\tan\beta$ allowed by the limit imposed on M_h. For values of the stop mass splitting of order 400 GeV or larger, the minimal value of $\tan\beta$ is obtained for $|\sin 2\theta_{\tilde{t}}| < 1$ and, therefore, the left- and right-handed stop mass parameters $M_{\tilde{t}_L}$, $M_{\tilde{t}_R}$ begin to differ, but the value of $\tilde{A}_t$ always remains larger than $M_{\tilde{t}_2}$, in agreement with our discussion above. We have also verified that the values of $\tilde{A}_t$ that maximize the Higgs boson mass, after the dominant leading logarithm two-loop corrections to the effective potential are included, are in good agreement with the ones obtained from the one-loop expression, Eqs. (4) and (6).

In the same figure we also show the bounds on $\tan\beta$, obtained from the requirement of perturbative consistency of the theory up to the grand unification scale [3] $M_{GUT} \simeq 2 \times 10^{16}$ GeV. In the MSSM, for sufficiently large values of the top-quark Yukawa coupling at the GUT scale, its low-energy values are governed by the quasi-infrared fixed-point solution [3]

$$\left(h_t^2(Q)\right)_{IR} \simeq \frac{8}{9} g_3^2(Q) \qquad \text{for } Q \sim \mathcal{O}(100\text{GeV}). \tag{12}$$

In order to obtain the physical top-quark mass, we compute the RG evolution of the Yukawa coupling from M_{GUT} down to the scale $Q = m_t$. The physical top-quark mass is then calculated by including all finite corrections in Eq. (1). The SM part of the corrections to Eq. (1) is dominated by the gluon contribution and, at the scale $Q = m_t$, is known up to $\mathcal{O}(\alpha_s^2)$ [16]. The corresponding SM one-loop corrections to Eq. (1) proportional to the top-quark Yukawa coupling are small, of the order of the two-loop QCD ones[17]. The one-loop supersymmetric particle corrections to Eq. (1) have been calculated in [18], and their relevance for the correct definition of the

[2] The Higgs boson mass bound quoted here has been obtained from a combined analysis of three of the four LEP experiments. The individual ALEPH analysis, not included in the combination, leads to a bound of order 87.9 GeV. The combination of the Higgs search data of the four experiments would lead to a slightly larger value of the Higgs mass bound, of order M_Z [15].

[3] The dependence of the lower bound on $\tan\beta$ on the precise value of M_{GUT} and $\alpha_s(M_Z)$ (we use $\alpha_s(M_Z) = 0.118$) is not significant for our purpose.

infrared fixed point solution has been stressed in Refs. [19, 6]. For values of the heavier stop mass and/or gluino masses much larger than the top-quark mass, they are dominated by two terms: the first contains large logarithmic factors, which can as well be taken into account by introducing appropriate step functions in the RGEs [20]:

$$\frac{d}{dt}h_t^2 \simeq \frac{h_t^2}{(4\pi)^2}\left\{\left[\frac{9}{2}+\theta_{\tilde{Q}}+\frac{1}{2}\theta_{\tilde{U}}\right]h_t^2-\left[8-\frac{4}{3}\left(\theta_{\tilde{Q}}+\theta_{\tilde{U}}\right)\theta_{\tilde{g}}\right]g_3^2\right\} \tag{13}$$

$$\frac{d}{dt}g_3^2 = \frac{g_3^4}{(4\pi)^2}\left\{-7+2\theta_{\tilde{g}}+\frac{1}{2}\left[2\theta_{\tilde{Q}}+\theta_{\tilde{U}}+\theta_{\tilde{D}}\right]\right\}, \tag{14}$$

where $t = \log(Q^2/M_Z^2)$, $\theta_{\tilde{X}} = \theta(Q - M_{\tilde{X}})$ and $\tilde{Q}$, $\tilde{U}$ and $\tilde{D}$ stand for the left-handed doublet, right-handed up and right-handed down squarks respectively. For simplicity, we have assumed that the squark masses are generation independent. When the logarithmic factors are large, they must be resummed, which we have done in our computations [21]. The second dominant term contains the non-logarithmic effects,

$$\frac{\delta m_t}{m_t} \simeq -\frac{2\alpha_3}{3\pi}\tilde{A}_t m_{\tilde{g}} \times I(m_{\tilde{g}}^2, M_{\tilde{t}_1}^2, M_{\tilde{t}_2}^2), \tag{15}$$

where

$$I(a,b,c) = \frac{a\ b\ \log(a/b) + a\ c\ \log(c/a) + b\ c\ \log(b/c)}{(a-b)\ (b-c)\ (a-c)} \simeq \mathcal{O}\left(\frac{1}{\max(a,b,c)}\right). \tag{16}$$

From the above expressions, the dependence of $\tan\beta$ obtained at the infrared fixed point solution on the sparticle spectrum may be qualitatively understood. For instance, if all supersymmetric particle masses take equal values $M_{\rm SUSY} \gg m_t$, the running of the top quark Yukawa coupling from the scale $M_{\rm SUSY}$ to the scale $Q \sim \mathcal{O}(m_t)$ will be governed by Eqs. (13), (14) with all $\theta_{\tilde{X}} = 0$. In this case the top quark Yukawa coupling becomes smaller at high energies compared to the case in which sparticles are light (all $\theta_{\tilde{X}} = 1$ from $Q \sim \mathcal{O}(m_t)$ up to $Q = M_{GUT}$), because in the former case the coefficients in Eq. (13) between $Q = m_t$ and $Q = M_{\rm SUSY}$ cause a slower increase of h_t. This implies a smaller lower bound on $\tan\beta$ for heavier sparticles. The mass of the gluino also has important effects on the bounds: if it is much lower than the stop masses, it makes the strong gauge coupling less asymptotically free in the low-energy effective theory, slowing the evolution of the top Yukawa coupling to large values with respect to the case $m_{\tilde{g}} \approx M_{\tilde{t}_i}$, implying again a smaller lower bound on $\tan\beta$. On the other hand, the gluino mass also controls the non-leading logarithmic corrections, Eq. (15), which become larger for heavier gluinos and larger values of the stop mixing parameters and, in certain regions of parameter space, can be

of the order of or larger than the leading-logarithmic corrections. In Fig. 1 we plot the maximal and minimal values of $\tan\beta$ at the fixed-point solution, which are obtained for a heavy gluino mass, of the order of the heavier stop one, and for $\sin 2\theta_{\tilde{t}} = \pm 1$, and also for heavy and light gluinos when the stop mass splitting vanishes.

The comparison of the lower bounds on $\tan\beta$ obtained from the lower limits on M_h and from perturbativity of the top Yukawa coupling is striking. In order to interpret the results correctly one should take into account that, for the same stop mass splitting, the bounds on $\tan\beta$ coming from the limits on the Higgs boson mass move rapidly up when the mixing parameter $|\tilde{A}_t|$ is lowered, while the bound set by the perturbativity of the top Yukawa coupling moves down (up) for positive (negative) values of $\tilde{A}_t$ (by definition $m_{\tilde{g}} > 0$). Already with the present lower limit on the Higgs boson mass, and for $M_{\tilde{t}_2} \lesssim 1$ TeV, the bounds on $\tan\beta$ coming from the experimental limit on M_h dominate over those coming from the perturbativity requirement, for values of the stop mass splitting smaller than 200 GeV (300 GeV) for positive (negative) values of the mixing angle. Only for larger values of the mass splitting in the stop sector viablefrared fixed-point solution of the top-quark mass be accessible. As shown in Fig. 2, these conclusions depend on the value of the top quark mass. If the top-quark mass were closer to 180 GeV, the bounds imposed by the Higgs mass limits would become weaker, enlarging the parameter space consistent with the infrared fixed-point solution. If, instead, the top-quark mass were closer to 170 GeV, the infrared fixed point solution would be even more constrained.

To discuss how natural are the large values of the mixing parameters needed to reach the infrared fixed point solution, consider the case where supersymmetry breaking is transmitted to the observable sector at scales of order M_{GUT}. In this case, the infrared fixed-point solution of the top-quark mass implies also an infrared fixed point in the parameters A_t and $\overline{m}^2 \equiv m_Q^2 + m_U^2 + m_{H_2}^2$ [5, 22, 6]

$$A_t \approx -1.5 M_{1/2} \qquad\qquad \overline{m}^2 \approx 6 M_{1/2}^2, \tag{17}$$

at scales of the order of the weak scale, where we have assumed a common value $M_{1/2}$ for the gaugino masses at M_{GUT} (useful formulae for the most general case can be found in [23, 24]). For the Higgs potential mass parameter $m_{H_2}^2$, one gets from the renormalization group evolution $m_{H_2}^2 \simeq -3M_{1/2}^2 + ...$, while the left- and right-handed stop mass parameters increase with $M_{1/2}$, $m_Q^2 \simeq 5.5 M_{1/2}^2 + ...$, $m_U^2 \simeq 3.5 M_{1/2}^2 + ...$, where the ellipses denote a dependence on the values of the stop and Higgs mass parameters at the scale M_{GUT}. Hence, increasing the stop masses and/or the gaugino masses, tends to produce large negative values of $m_{H_2}^2 \approx -0.5\mathcal{O}(M_{\tilde{t}_i}^2)$ [4]. Combining

[4] This can only be avoided by having very large values of the scalar mass parameters

these solutions with the condition of electroweak symmetry breaking, one finds that large values of $\tilde{A}_t$ can be naturally obtained at the fixed point. In such cases, however, these large values of $\tilde{A}_t$ are negative, implying that the values of $\tan\beta$ associated with the infrared fixed point solutions move to lower values compared to the case of no mixing.

Figure 3 shows the bounds on $\tan\beta$ that will be obtained in the case that no Higgs boson signal is found at LEP for $\sqrt{s} = 192$ GeV, implying a bound $M_h \gtrsim 98$ GeV [25] [5]. In that case, even for large values of the stop mass splitting and the mixing parameter, the bound on $\tan\beta$ resulting from the Higgs mass constraints will be stronger than the perturbativity bounds for values of the heavier stop mass smaller than 700 GeV (1 TeV), for positive (negative) values of the stop mixing angle. Hence, as was already emphasized in different works, a run of LEP at $\sqrt{s} = 192$ GeV will test most of the parameter space consistent with the infrared fixed-point solution [3, 22, 6] for a top-quark mass $m_t^{pole} \lesssim 175$ GeV.

Finally, Fig. 3 also shows the bounds that will apply after the final run of LEP, at $\sqrt{s} = 200$ GeV, assuming a potential lower limit on the Higgs boson mass of order 108 GeV [25]. It is clear that only moderate or large values of $\tan\beta$ will be allowed if the Higgs boson is not found at the final run of LEP. This will provide a strong motivation for $SO(10)$-type unification models, in which large values of $\tan\beta$ and Higgs masses of order $110 - 120$ GeV are naturally predicted [26]. Of course, from Figs. 1 and 3, one can also infer the values of the stop mass parameters consistent with the infrared fixed-point solution of the top-quark mass, in the case that the Higgs boson is found at the future runs of the LEP collider.

Up to now we have been discussing the situation with a large CP-odd Higgs boson mass, $M_A \gg M_Z$. Since for the other MSSM parameters fixed, M_h is maximal for $M_A \gtrsim 250$ GeV, this is the configuration that is expected to yield the smallest lower bound on $\tan\beta$. Indeed, for smaller values of M_A (for a fixed stop spectrum and fixed value of $\tan\beta$) both the coupling to the Z^0 boson and the mass of the lighter CP-even Higgs particle decrease. For $\tan\beta \lesssim 3$ and 150 GeV$\lesssim M_A \lesssim 250$ GeV, the decrease of M_h compensates the drop in the $h^0 Z^0 Z^0$ coupling, so that the Higgs boson strahlung cross section actually increases, implying a bound on $\tan\beta$ stronger than that obtained for $M_A \gtrsim 250$ GeV [25]. For values of $M_A \lesssim 130$ GeV and values of $\tan\beta \gtrsim 4$, however, this ceases to be true. In this regime, the $h^0 A^0$ associated production cross section rapidly increases, and this becomes the most efficient channel for supersymmetric Higgs boson detection. Hence, a small window for $M_A \simeq \mathcal{O}(100$ GeV) may still exist, for which the lower bound on $\tan\beta$ for a given stop spectrum may be lower than the ones presented in

at the GUT scale, with very specific correlations between them [22, 23].

[5] As emphasized above, in the numerical computations we have lowered the bound by 2 GeV with respect to the considered Higgs mass limit

this work (see also [29]) [6]. Since this window tends to occur for relatively large values of $\tan\beta$, for which precise determination of the bounds would require exploration of the full Higgs boson discovery potential at LEP (and combination of the results of the four LEP collaborations at the next runs of LEP), we shall not explore this possibility within this work.

It is also instructive to study the impact of precision electroweak measurements on the stop mass limits derived above. In Fig. 4, we compare for $\tan\beta = 1.5$ and $m_t = 175$ GeV (close to the infrared fixed point), and three different values of the lighter stop mass $M_{\tilde{t}_1}$, the regions in the $(M_{\tilde{t}_2},\ \theta_{\tilde{t}})$ plane allowed by the present limit on the Higgs boson mass[7] (solid lines) and by precision measurements (shadowed area). To be conservative the precision data constraints are taken into account by requiring $\Delta^{stops}\rho \lesssim 6 \times 10^{-4}$) [1]. The precision measurement bounds are clear: for $\theta_{\tilde{t}} = 0$ (corresponding to purely right-handed lighter stop), the mass of the heavier (left-handed) stop is bounded from below (coming from the imposed bound on $\Delta\rho$), but no upper bound can be set. For values of $\theta_{\tilde{t}} \simeq \pi/2$, the constraint on $\Delta\rho$ can be satisfied only by tuning the value of $\tilde{A}_t$ to be large and of the order of the right-handed stop mass [27, 28]. For $\sin 2\theta_{\tilde{t}} \simeq 1$, precision measurements put an upper bound on the heavier stop mass, which, for sufficiently large splitting of the stop masses, can be lower than the lower bound obtained from the limits on the Higgs boson mass. Hence, for a given value of the heavier stop mass a non-trivial bound on the lighter stop mass can be obtained. In particular, we see from Fig. 4 that for values of $\tan\beta$ close to the fixed point and values of the mixing that maximize the Higgs-boson mass, precision measurements disfavours values of the lighter stop mass below 150 GeV. Notice, however, that acceptable values of the parameter $\Delta\rho$ can be obtained by increasing the heavier (or the lighter) stop mass. In particular, close to the fixed point, and for values of the lighter stop mass above 150 GeV, the bounds on the stop parameters imposed by the limits on the Higgs boson mass become stronger than the ones coming from precision data (the opposite is true for large values of $\tan\beta$ [28]).

A striking result that appears from Fig. 4 is the existence of an effective upper bound on the heavier stop mass (for fixed $\theta_{\tilde{t}}$) from the present limit on the Higgs boson mass. It is interesting to understand the situation for values of $\sin 2\theta_{\tilde{t}} \simeq 1$, for which the largest values of the Higgs boson mass are obtained. In this case, the mixing parameter is approximately given by

$$\tilde{A}_t \simeq \frac{M^2_{\tilde{t}_2} - M^2_{\tilde{t}_1}}{2m_t}. \tag{18}$$

[6] This depends, however, on the other details of the MSSM spectrum, since, in this case, constraints from $b \to \gamma s$ and $Z^0 \to \bar{b}b$ come into play.

[7] As explained before, we take $M_h > 88\,\mathrm{GeV}$ as a conservative estimate in our numerical computation.

This means that the ratio $\tilde{A}_t/M_{\rm SUSY} \equiv \tilde{A}_t/M_{\tilde{t}_2}$ grows as $M_{\tilde{t}_2}/m_t$ for growing $M_{\tilde{t}_2}$, leading, by Eqs. (8), (9), to negative contributions to M_h, which rapidly overcome the positive logarithmic dependence on $M_{\tilde{t}_2}$. For very large stop mass splitting, of course, Eq. (8) is not applicable, and the exact value should be obtained by using the whole renormalization group improved effective potential [11].

As emphasized above, the perturbativity bounds depend also on the physics at scales larger than the supersymmetric particle masses and, hence, are model-dependent. Adding new matter multiplets with non-trivial $SU(3)\times SU(2)\times U(1)$ quantum numbers at some intermediate scale M_I, e.g. extra $\mathbf{5}+\bar{\mathbf{5}}$ and/or $\mathbf{10}+\overline{\mathbf{10}}$ matter representations (having no interactions with the ordinary matter in the superpotential), decreases the lower perturbativity limit on $\tan\beta$. This is easy to understand, by noting that above the scale M_I, α_s becomes less asymptotically free (i.e. goes up steeper) and, therefore, has a stronger damping effect on the top quark Yukawa coupling, thus allowing for a larger initial value at $Q = m_t$ (and, hence, lower $\tan\beta$). Of course, adding more extra representations at lower scale M_I allows for smaller $\tan\beta$. One could hope, therefore, that with a suitable number of extra representations at some scale M_I one can reach a lower limit on $\tan\beta$ smaller than 1 and at the same time satisfy also the Higgs mass limit (see Fig. 1). However, for a given scale M_I the number of extra representations is limited by perturbativity of the gauge couplings. With all one-loop threshold corrections to the relation (1) we find that for $M_I \gtrsim 10^5$ GeV one can afford at most five $\mathbf{5}+\bar{\mathbf{5}}$ representations (or two $\mathbf{5}+\bar{\mathbf{5}}$ and one $\mathbf{10}+\overline{\mathbf{10}}$ representations) for relatively heavy ($\gtrsim 1.5$ TeV) sparticle spectra. For sparticle spectra $\lesssim 1$ TeV only four $\mathbf{5}+\bar{\mathbf{5}}$ representations (or one $\mathbf{5}+\bar{\mathbf{5}}$ and one $\mathbf{10}+\overline{\mathbf{10}}$ representations) are allowed. As a result, the perturbativity limit on $\tan\beta$ can approach 1 only for very heavy sparticle spectra ($\gtrsim 2$ TeV) and/or large mixing stop mass parameters. This is illustrated in Fig. 5.

In very interesting works [30, 31], it has been shown that, in the minimal supergravity model, the infrared fixed-point solution is already ruled out by the requirement of having a phenomenologically acceptable amount of dark matter and/or avoiding charge- or colour-breaking minima. It is important to notice, however, that in general supergravity models, the masses of sfermions with different quantum numbers may be different. In particular, there might be no correlation between the slepton, Higgs, neutralino and squark masses. Without these correlations, it is difficult to relate the neutralino annihilation cross section to the Higgs and stop spectrum and hence, the fixed-point solution cannot be ruled out by these considerations. Moreover, even if the correlations between sparticle masses were similar to the ones present in the minimal supergravity model, a tiny violation of R-parity would be sufficient to suppress these cosmological constraints on the infrared fixed-point solution and to avoid dangerous colour- or charge-breaking minima [31].

In another independent work, it has been noted [32] that the amount of fine tuning [33] increases for low values of $\tan\beta$ close to the fixed-point. This is specially the case for the large values of the stop masses that are necessary to approach the fixed-point solution. If a Higgs particle is found in the next runs of the LEP collider, it would be interesting to investigate the conditions necessary to obtain a spectrum consistent with the fixed-point solution in a natural way. If it is not found, the fixed-point solution will be ruled out by solid experimental data.

Another cosmologically interesting scenario, which demands Higgs masses in the range of LEP2, is electroweak baryogenesis [34]. The realization of this scenario, however, demands a light stop and relatively small values of the stop mixing. As follows from the present analysis of the constraints on the stop sector imposed by the Higgs boson mass limits (and precision data), the above requirements can only be satisfied either for moderate values of $\tan\beta$, or for very large values of the heavier stop mass. In fact, for values of the heavier stop mass at most of the order of 2 TeV, a lower bound on $\tan\beta \gtrsim 2$ can already be obtained in this particular case. Hence, this scenario is not consistent with the infrared fixed-point solution.

Let us finish this discussion by mentioning that in this work we have assumed the absence of any extra Higgs-like states in the low-energy spectrum. For instance, the presence of a singlet [35], with a tree-level superpotential coupling $\lambda S H_1 H_2$ would induce a tree-level quartic coupling for the lighter CP-even Higgs boson proportional to $\lambda^2 \sin^2 2\beta$ [36]. This tree-level contribution would become most important for low values of $\tan\beta$ and could only be constrained by perturbativity limits on the coupling λ. If such a singlet were present in the low-energy spectrum, the bounds on $\tan\beta$ and on the stop mass parameters would be considerably modified.

Acknowledgements The work of P. Ch. and S. P. has been partly supported by the Polish State Committee for Scientific Research grant 2 P03B 030 14. M.C. and C.W. would like to thank J.R. Espinosa, S. de Jong, P. Janot, H. Haber, P. Igo-Kemenes and G. Weiglein for useful discussions.

References

[1] J. Erler and D.M. Pierce, preprint SLAC-PUB-7633 (hep-ph/9801238).

[2] D. Reid, talk at XXXIII Rencontres de Moriond (Electroweak Interactions and Unified Theories), Les Arcs, France, March 1998; LEP Electroweak Working Group, report LEPEWWG/97-01.

[3] B. Pendleton and G.G. Ross, *Phys. Lett.* **98B** (1981) 21; C.T. Hill, *Phys. Rev.* **D24** (1981) 691; C.T. Hill, C.N. Leung and S. Rao, *Nucl. Phys.* **B262** (1985) 517.

[4] The CDF Collaboration, F. Abe et al., *Phys. Rev. Lett.* **74** (1995) 2676; The D0 Collaboration, S. Abachi et al., *Phys. Rev. Lett.* **74** (1995) 2632; R. Raja (for the D0 and CDF Collaborations), talk at XXXII Rencontres de Moriond (Electroweak Interactions and Unified Theories), Les Arcs, France, March 1997, FERMILAB-CONF-97-194-E (hep-ex/970611); M. Jones (for the D0 and CDF Collaborations) talk at XXXIII Rencontres de Moriond (Electroweak Interactions and Unified Theories), Les Arcs, France, 1998.

[5] M. Carena, M. Olechowski, S. Pokorski, C.E.M. Wagner, *Nucl. Phys.* **B419** (1994) 213;

[6] J.A. Casas, J.R. Espinosa and H.E. Haber, preprint IEM-FT-167-98 (hep-ph/9801365)

[7] H.E. Haber, in *Perspectives on Higgs Physics II*, ed. G.L. Kane, World Scientific, Singapore, 1998.

[8] R. Hempfling, Ph. D. thesis, UCSC preprint SCIPP 92/28 (1992); J. Ellis, G. Ridolfi and F. Zwirner, *Phys. Lett.* **257B** (1991) 83; *Phys. Lett.* **262B** (1991) 477; J.L. Lopez, D.V. Nanopoulos, *Phys. Lett.* **266B** (1991) 397.

[9] R. Hempfling and A. Hoang, *Phys. Lett.* **331B** (1994) 99;
J. Kodaira, Y. Yasui and K. Sasaki, *Phys. Rev.* **D50** (1994) 7035.

[10] J. Casas, J.R. Espinosa, M. Quiros and A. Riotto, *Nucl. Phys.* **B436** (1995) 3.

[11] M. Carena, J.-R. Espinosa, M. Quiros and C.E.M. Wagner, *Phys. Lett.* **355B** (1995) 209; M. Carena, M. Quiros and C.E.M. Wagner, *Nucl. Phys.* **B461** (1996) 407.

[12] H. Haber, R. Hempfling and A.H. Hoang, *Z. Phys.* **C57** (1997) 539.

[13] S. Heinemeyer, W. Hollik and G. Weiglein, preprint KA-TP-2-1998 (hep-ph/9803277).

[14] ALEPH Collaboration, *Preliminary Limits from Searches for Neutral Higgs Bosons in e+e- Collisions at Centre-of-mass Energies of 181-184 GeV*, ALEPH 98-029 CONF 98-017; DELPHI Collaboration, *DELPHI Results at 183 GeV*, presented by Klaus Moenig, LEPC Meeting, CERN, March 31, 1998; L3 Collaboration, *Search for the Standard Model*

Higgs Boson in e+e- Interactions at $\sqrt{s}$ *= 183 GeV*, M. Acciarri et al., preprint CERN-EP/98-052; OPAL Collaboration, *Search for Neutral Higgs Bosons in e+e- Collisions at sqrt(s)=183 GeV*, OPAL Physics Note PN340, 9th March 1998; V. Ruhlmann-Kleider, *Search for Higgs bosons at LEP200*, in Proc. of the XXX1st Rencontres de Moriond (QCD and high energy interactions), Les Arcs, March 1998.

[15] P. Janot, private communication.

[16] N. Gray, D.J. Broadgurst, W. Grafe and K. Schilcher, *Z. Phys.* **C48** (1990) 673.

[17] R. Hempfling and B.A. Kniehl, *Phys. Rev.* **D51** (1995) 1386.

[18] D.M. Pierce, hep-ph/9407202, *Proceedings of the International Workshop on Supersymmetry and Unification of Fundamental Interactions* (SUSY 94), eds. C. Kolda and J. Wells; J.A. Bagger, K. Matchev and D.M. Pierce, *Phys. Lett.* **248B** (1995) 443; J.A. Bagger, K. Matchev, D.M. Pierce and R. Zhang, *Nucl. Phys.* **B491** (1997) 3.

[19] N. Polonsky, *Phys. Rev.* **D54** (1996) 453.

[20] D.J Castaño, E.J. Piard and P. Ramond, *Phys. Rev.* **D49** (1994) 4882.

[21] P.H. Chankowski, in preparation.

[22] M. Carena and C.E.M. Wagner, *Nucl. Phys.* **B452** (1995) 45.

[23] M. Carena, P.H. Chankowski, M. Olechowski, S. Pokorski and C.E.M. Wagner, *Nucl. Phys.* **B491** (1997) 103;

[24] C.E.M. Wagner, preprint CERN-TH/98-21 (hep-ph/9801376).

[25] M. Carena, P. Zerwas and the Higgs Physics Working Group, *Physics at LEP2*, Vol. 1, eds. G. Altarelli, T. Sjöstrand and F. Zwirner, Report CERN 96-01 (1996).

[26] M. Carena, M. Olechowski, S. Pokorski and C.E.M. Wagner, *Nucl. Phys.* **B426** (1994) 269;

[27] M. Carena, D. Choudhury, S. Raychaudhuri and C.E.M. Wagner, *Phys. Lett.* **414B** (1997) 92.

[28] P.H. Chankowski preprint IFT/97-18 (hep-ph/9711470), to appear in *Proceedings of the Int. Workshop on Quantum Effects in the MSSM*, Barcelona, Spain, September 1997.

[29] OPAL Collaboration, CERN-EP/98-029, (hep-ex/9803019).

[30] J. Ellis, T. Falk, K. Olive and M. Schmitt, *Phys. Lett.* **388** (1996) 97 and preprint CERN-TH/97-105 (hep-ph/9705444).

[31] S.A. Abel and B.C. Allanach, hep-ph/9803476.

[32] P.H. Chankowski, J. Ellis and S. Pokorski, preprint CERN-TH-97-343 (hep-ph/9712234); R. Barbieri and A. Strumia, preprint IFUP-TH-4-98 (hep-ph/9801353).

[33] R. Barbieri and G.-F. Giudice, *Nucl. Phys.* **B306** (1988) 63; G.W. Anderson and D.J. Castaño, *Phys. Lett.***347B** (1995) 300; S. Dimopoulos and G.-F. Giudice, *Phys. Lett.* **357B** (1995) 573.

[34] M. Carena, M. Quiros and C.E.M. Wagner, *Phys. Lett.* **380B** (1996) 81.

[35] P. Fayet, *Nucl. Phys.* **B90** (1975) 104; H.-P. Nilles, M. Srednicki and D. Wyler, *Phys. Lett.* **120B** (1983) 346; J.-P. Derendinger and C.A. Savoy, *Nucl. Phys.* **B237** (1984) 307; M. Drees, *Int. J. Mod. Phys.* **A4** (1989) 3635.

[36] J. Ellis et al., *Phys. Rev.* **D39** (1989) 844; C. Savoy and P. Binetruy, *Phys. Lett.* **277B** (1992) 453; J.-R. Espinosa and M. Quiros, *Phys. Lett.* **279B** (1992) 92 and hep-ph/9804235; M. Masip, R. Munoz-Tapia and A. Pomarol, preprint UG-FT-84-97 (hep-ph/9801437).

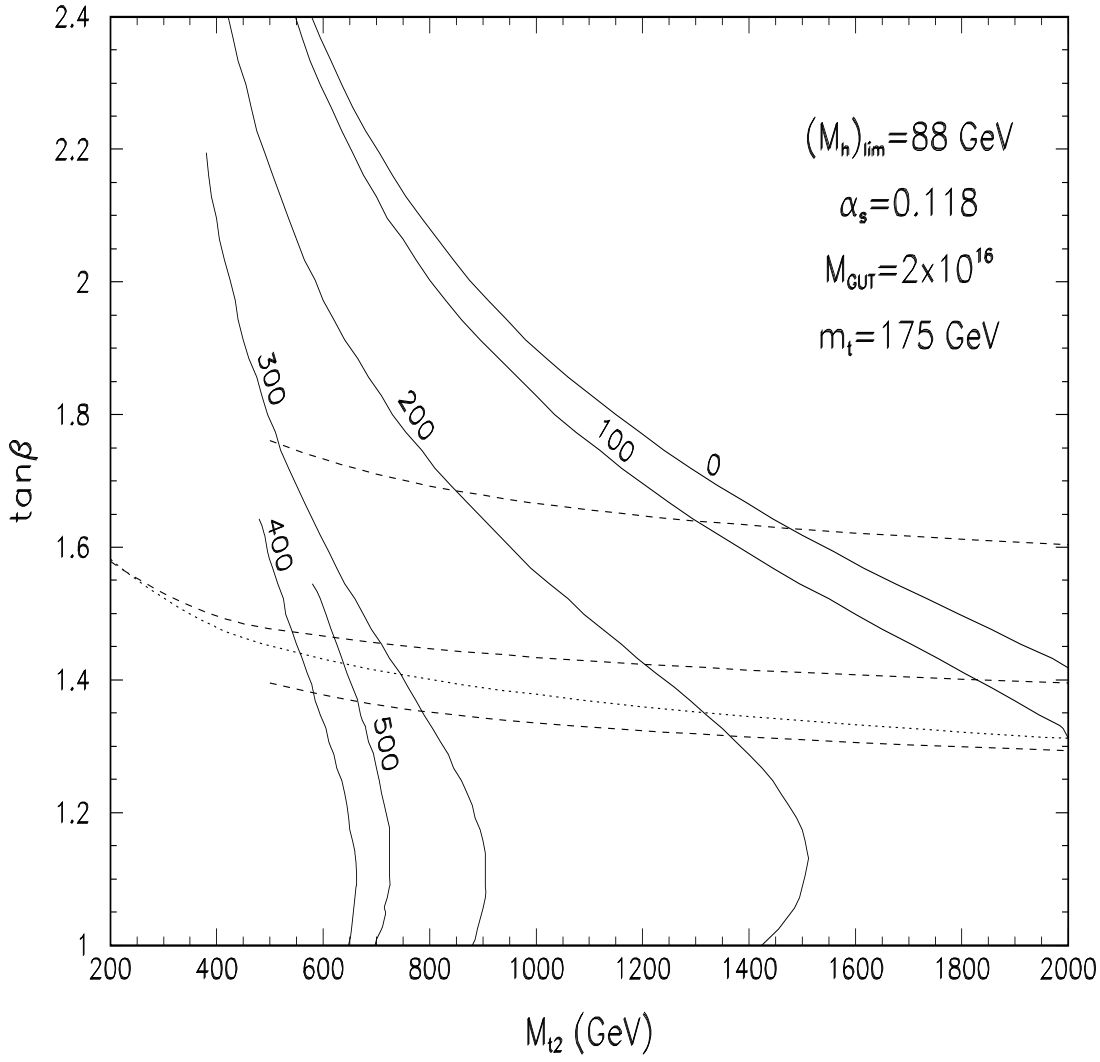

Figure 1: Bounds on $\tan\beta$ obtained for $m_t^{pole} = 175$ GeV and for a lower bound on the Higgs boson mass $M_h > 88$ GeV, as a function of the heavier stop mass, for different values of the stop mass splitting $\Delta M_{\tilde{t}} = 0$–500 GeV (solid lines). Also plotted here are the top Yukawa coupling perturbativity bounds for the case of heavy gluino ($m_{\tilde{g}} = M_{\tilde{t}_2}$) for $\Delta M_{\tilde{t}} = 400$ GeV and $\sin 2\theta_{\tilde{t}} = \pm 1$ (upper-lower dashed lines), and for heavy gluino (center-dashed lines) and light gluino ($m_{\tilde{g}} = 200$ GeV) (dotted line) for $\Delta M_{\tilde{t}} = 0$.

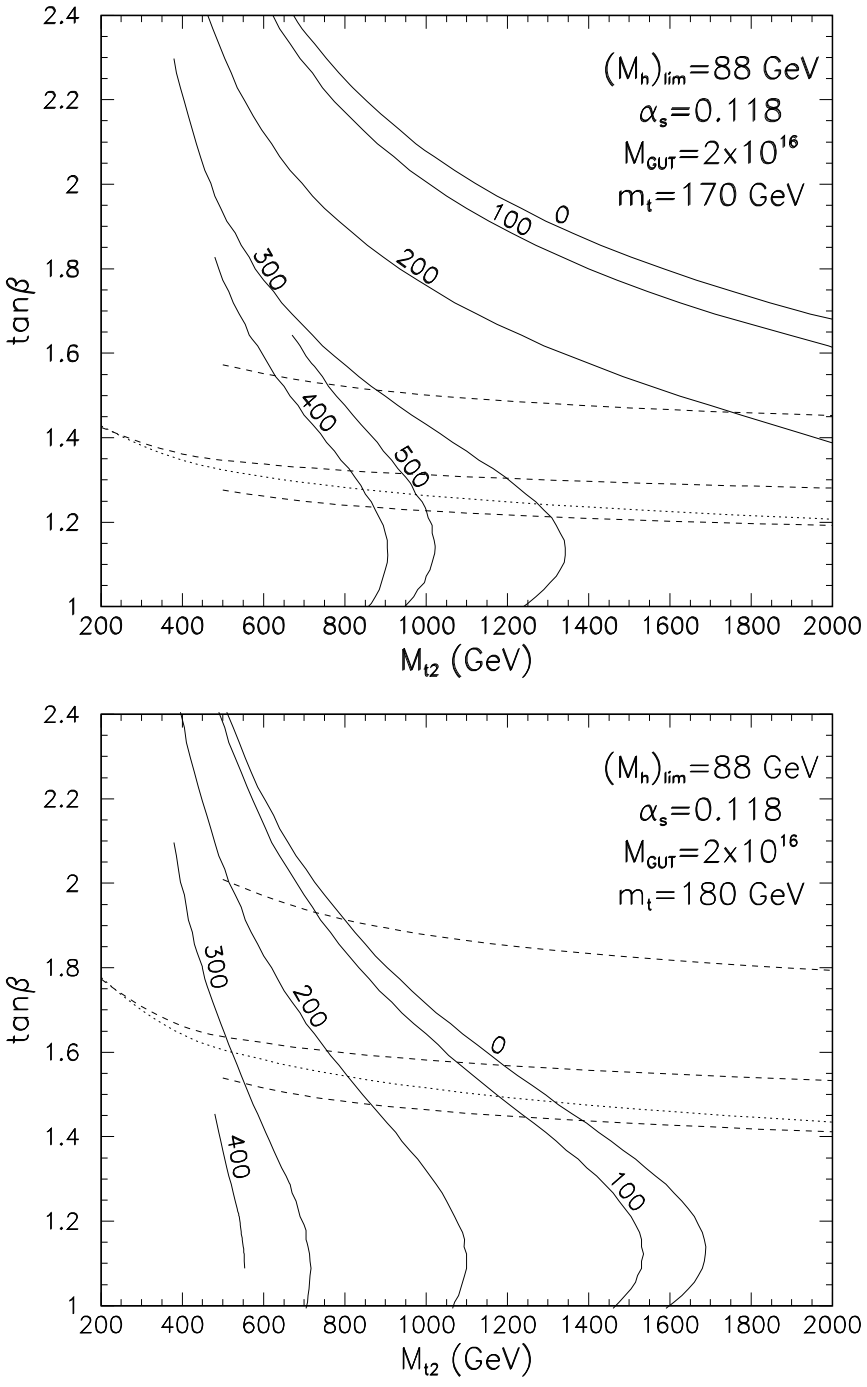

Figure 2: The same as Fig. 1, but for $m_t^{pole} = 170$ GeV and $m_t^{pole} = 180$ GeV.

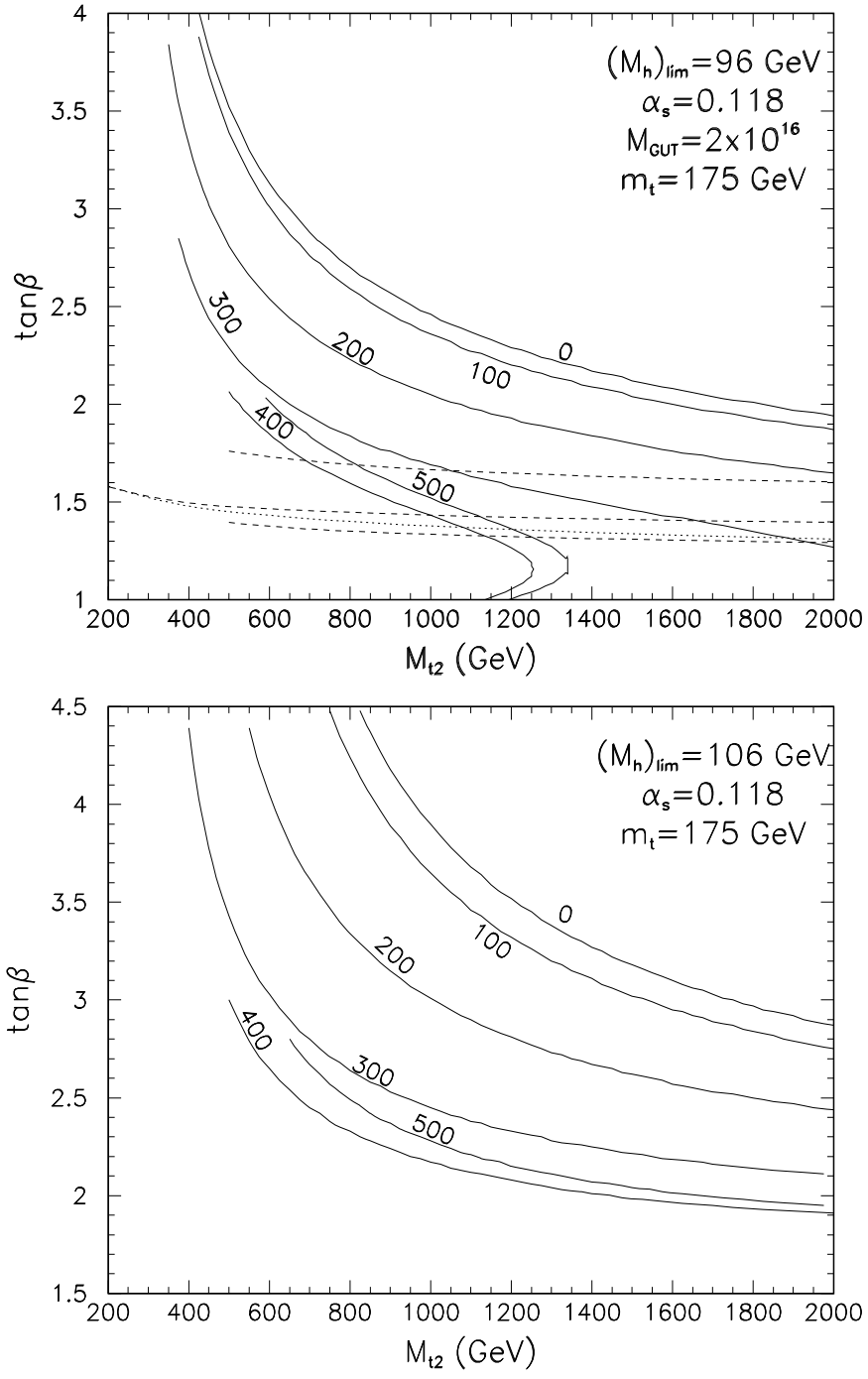

Figure 3: The same as Fig. 1, but for lower bounds on the Higgs boson mass of 96 GeV and 106 GeV.

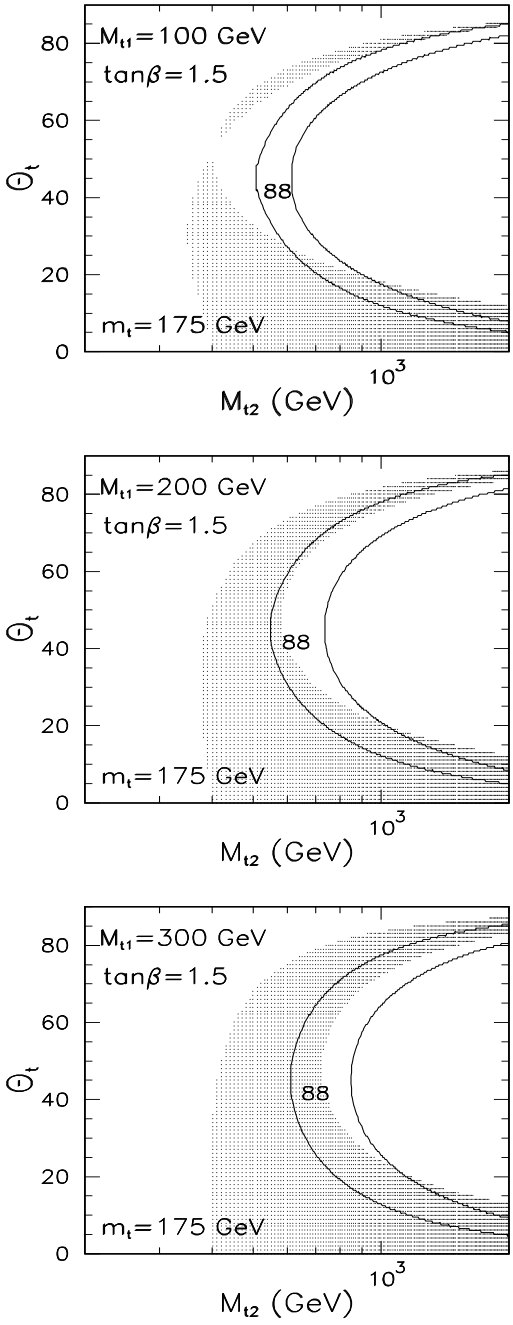

Figure 4: Bounds coming from the constraints on the parameter $(\Delta\rho)^{stops}$ (shadowed region) in the heavier stop mass–stop mixing angle plane, for values of $\tan\beta = 1.5$, and for different values of the lighter stop mass $M_{\tilde{t}_1} =$ 100, 200 and 300 GeV. Also shown here are the bounds obtained from the present limit on the Higgs boson mass (regions between solid lines).

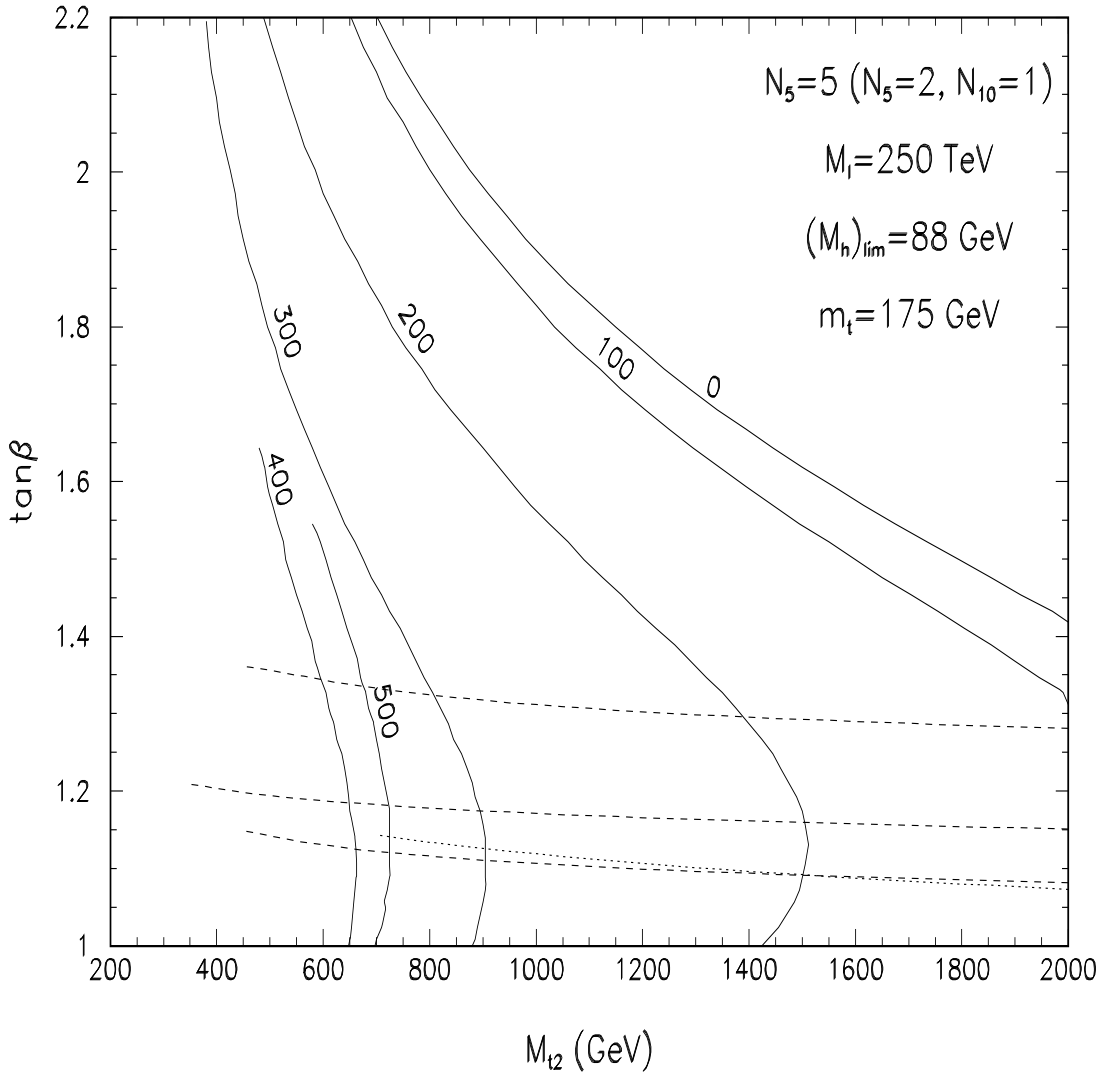

Figure 5: The same as Fig. 1, but with five additional $\mathbf{5} + \bar{\mathbf{5}}$ pairs (or equivalently, two $\mathbf{5} + \bar{\mathbf{5}}$ pairs and one $\mathbf{10} + \overline{\mathbf{10}}$ pair) added at the scale of 250 TeV.